Fresh Produce ©2009 Global Science Books

The Robustness of PLS Models for Soluble Solids Content of Mangosteen using Near Infrared Reflectance Spectroscopy

Sontisuk Teerachaichayut[1*] • Anupun Terdwongworakul[2] • Jutamas Phonudom[1] • Wanchaya Uamsatianporn[1]

[1] Department of Food-processing Engineering, Faculty of Agro-Industry, King Mongkut's Institute of Technology Ladkrabang, Ladkrabang, Bangkok 10520, Thailand
[2] Department of Agricultural Engineering, Faculty of Engineering at Kamphaeng Saen, Kasetsart University, Kamphaeng Saen Campus, Nakhonpathom 73140, Thailand

Corresponding author: * ktsontis@kmitl.ac.th

ABSTRACT

This research investigated the soluble solids content in translucent flesh which is an internal defect of mangosteen fruit (*Garcinia mangostana* L.). Near infrared (NIR) reflectance spectroscopy was used for the development of partial least squares calibration models for the prediction of the soluble solids content. Samples of 213 normal mangosteens and 87 translucent mangosteens were used for this experiment. Juice samples extracted from both normal flesh and translucent flesh were measured for their soluble solids contents. Diffuse reflectance spectra of juice samples were acquired in a range of 1100 to 2500 nm. In this research, a NIR spectrometer was able to predict the soluble solids content of mangosteen. The best model was developed with second derivative treatment. The calibration model of normal-flesh juice obtained high accuracy for prediction with a set of normal flesh samples (standard error of prediction (SEP) = 0.655, bias = 0.047) and poor accuracy for prediction with a set of translucent flesh samples (SEP = 1.245, bias = 0.224). The results indicate that NIR technology has high potential to develop calibration models for the prediction of the difference in quality of flesh in mangosteen.

Keywords: internal defect, NIR, prediction, quality, translucent flesh

INTRODUCTION

Mangosteen is called the "queen of the tropical fruits" because it is considered to be one of the most popular and delicious fruits. The edible aril is white, soft and juicy with a luscious and slightly acid taste (Martin 1980). Translucent flesh in mangosteen where the soft-white flesh changes to crisp-translucent flesh is an internal disorder. It may occur from nutrient imbalance and excessive water uptake into the flesh or mechanical injuries (Pankasemsuk *et al*. 1996). This defect makes quality unacceptable for export. Therefore, a reliable and high accuracy technique for translucent flesh detection is required.

In recent years, soluble solids content (SSC) has been chemical data commonly used for assessing quality of fruits by NIR spectroscopy such as cantaloupe (Dull *et al*. 1989), melon (Dull *et al*. 1992), peach (Kawano *et al*. 1992), mandarin (Kawano *et al*. 1993), apple (Ventura *et al*. 1998), kiwifruit (McGlone *et al*. 1998), prune (Slaughter *et al*. 2003) and mango fruit (Saranwong *et al*. 2003). A number of investigations have compensated for the effect of growing seasons. Peirs *et al*. (2003) used NIR reflectance spectroscopy to analyze the effect of orchard, season and cultivar on the robustness of calibration models for SSC of apples. Sohn (2001) applied NIR reflectance spectroscopy to develop calibration models for sweetness determination of Fuji apple with different growing districts and harvest years. As for detection of defects in fruit, Teerachaichayut *et al*. (2007) used an NIR transmittance spectrometer to qualitatively evaluate intact mangosteens for translucent flesh detection by using the difference in absorbance.

This study investigated the prediction of the SSC in mangosteeen flesh from the normal and translucent aril. The difference in SSC between the normal and translucent flesh was emphasized.

MATERIALS AND METHODS

Fruit samples

A set of 300 mangosteen samples from a Thai local fruit auction was used for this study. The samples were transported to the laboratory and stored in an air-conditioned room under 25°C for about 12 h prior to the measurements. The samples were cut open and photographed to record internal visible flesh appearance as shown in **Fig. 1**. Then the quality of each fruit was inspected and judgement was made to assign the samples to a group of normal flesh (N = 213) or a group of translucent flesh (N = 87).

Fig. 1 Example of different internal quality of mangosteens expressing normal flesh (**A**) and translucent flesh (**B**).

Chemical analysis

The whole flesh was removed from its peel and juice extracted using a manual fruit squeezer. Each juice sample was filtered in order to separate the dispersed solid particles. The juice from each sample was measured for the soluble solids content (SSC) with a digital refractometer (PR101, Palette Series, Atago Co., Ltd., Tokyo, Japan).

Received: 17 December, 2008. Accepted: 21 May, 2009.

Original Research Paper

Table 1 Description of calibration and prediction sample sets of mangosteen juice.

Sample group	Set	N	Range	Mean value	Standard deviation	Unit
Overall juice	Calibration	200	10.8-21.6	17.36	1.916	°Brix
	Prediction	100	11.9-21.2	17.34	1.867	°Brix
Normal-flesh juice	Calibration	143	11.9-21.6	17.67	1.796	°Brix
	Prediction	70	12.0-21.0	17.64	1.712	°Brix
Translucent-flesh juice	Calibration	57	10.8-20.0	16.57	2.05	°Brix
	Prediction	30	11.8-19.4	16.67	1.959	°Brix

Table 2 Results of preprocessing for PLSR models using combined juice.

	Calibration PLSR model				Prediction					
					Normal-flesh juice (N = 70)			Translucent-flesh juice (N = 30)		
	N	LV	R	SEC	R	SEP	Bias	R	SEP	Bias
Normal-flesh juice	143	6	0.966	0.462	0.935	0.655	0.047	0.812	1.245	0.224
Translucent-flesh juice	57	7	0.964	0.546	0.791	1.071	-0.605	0.831	1.134	-0.166
Combined juice	200	6	0.945	0.634	0.947	0.553	0.052	0.863	1.027	0.122

N is number of samples
LV is the number of latent variables chosen for the calibration model
R is multiple correlation coefficients
SEC is standard error of calibration
SEP is standard error of prediction

Spectral acquisition

The filtered juice from each sample was introduced into a sample cell and the NIR spectra were immediately measured using a grating near infrared (NIR) reflectance spectrometer (InfraAlyzer 500, Bran+Luebbe, Norderstedt, Germany). The spectrometer was installed with PbS detector in the region of 1100 to 2500 nm (with 2 nm increments). The average spectrum of 2 repeated spectra measured for each sample was used for the evaluation.

Data analysis

Three data sets were created for analysis in this study. They consisted of combined juice group, normal-flesh juice group, and translucent-flesh juice group. The combined juice group of 300 samples was randomly divided into 200 samples for a calibration set and 100 samples for a prediction set having similarly distributed SSC. The normal-flesh juice sub-group of 213 samples was divided into 143 samples for a calibration set and 70 samples for a prediction set. Finally, the translucent-flesh juice sub-group of 87 samples was divided into 57 samples for a calibration set and 30 samples for a prediction set.

For each data set, partial least squares regression (PLSR) was performed to obtain models using the calibration sets and validated using the validation sets. The pre-processing procedures to the acquired spectra were investigated so as to establish the optimum calibration model. Cross-validation was used to evaluate the quality of the calibration model. The standard error of calibration (SEC) with cross validation was investigated to choose the number of latent variables (LV) in the calibration model. The SSC measurements, the predicted values, the correlation coefficient and the standard error of prediction (SEP) were used to judge the predictive performance of the calibration models. Cross-predictions of the calibration models were also performed and the results of the cross-predictions were compared using SEP to judge the difference, relation and accuracy of the models among groups. Data were analyzed using 'The Unscrambler' (version 9.6, CAMO AS, Trondheim, Norway), the statistical program for multivariate calibration.

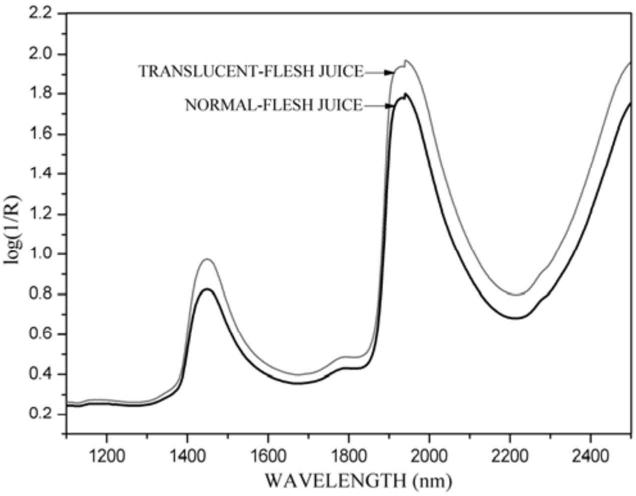

Fig. 2 Averaged original spectra of normal-flesh juice and translucent-flesh juice.

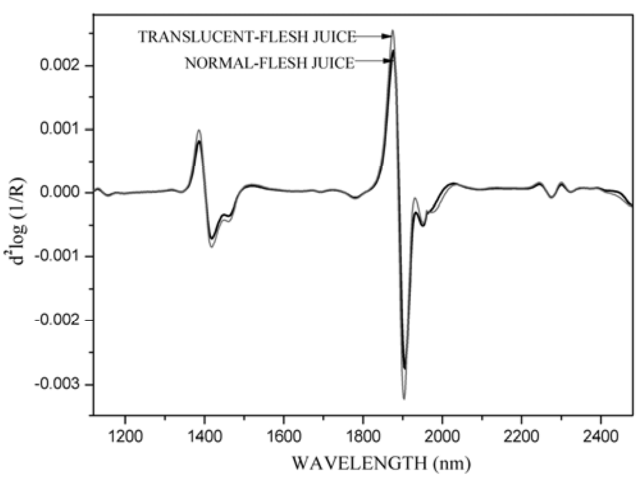

Fig. 3 Averaged second-derivative spectra of normal-flesh juice and translucent-flesh juice.

RESULTS AND DISCUSSION

The characteristics of samples in each group are shown in **Table 1**. The mean Brix value of translucent-flesh juice was lower than the mean Brix value of normal-flesh juice. However, in the perspective of standard deviation, an overlap of Brix value was observed.

NIR spectra

The average NIR spectra from the group of normal-flesh juice and the group of translucent-flesh juice are shown in **Fig. 2**. The spectrum characterizing the translucent-flesh juice was higher in absorbance than that of normal-flesh juice. This agreed with a previous investigation (Teerachaichayut *et al.* 2007), though from a different mode of measurement, that the translucency in mangosteen led to greater transmission of NIR light.

The optimal data preprocessing algorithms of second-derivative transformation were found to give the optimum performance. Representative second-derivative spectra of

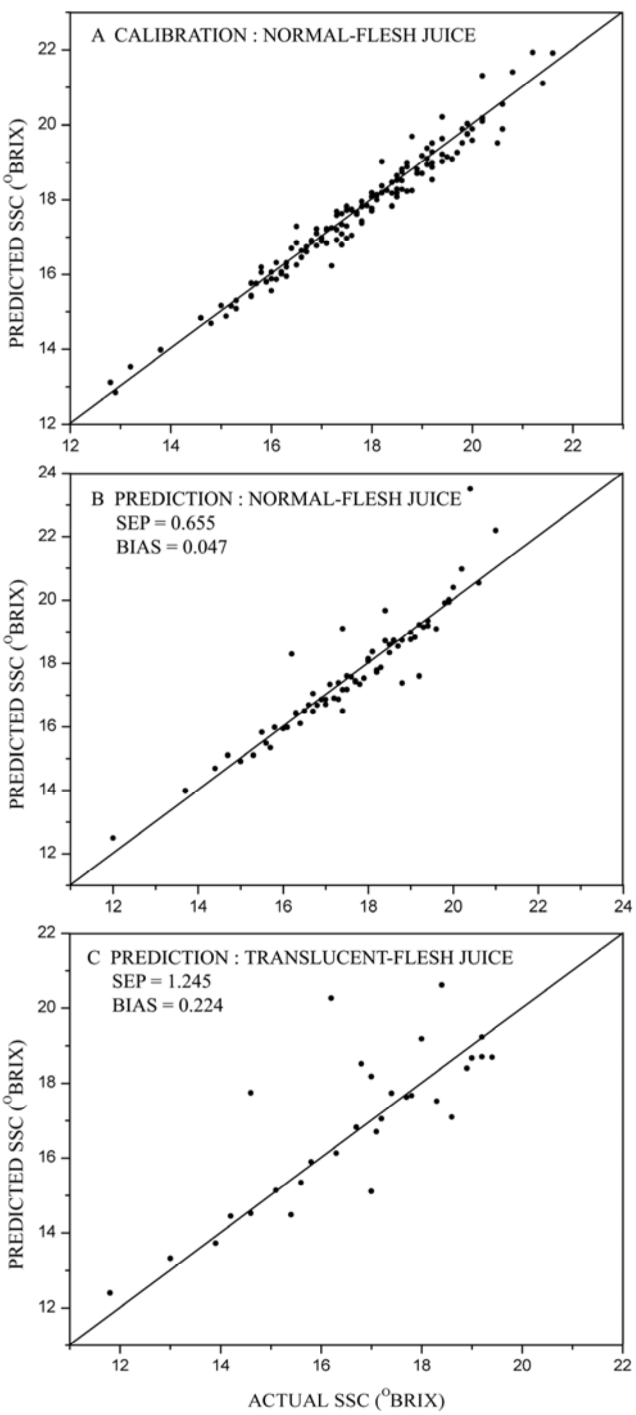

Fig. 4 Scatter plots of actual SSC and predicted SSC for the calibration set of normal-flesh juice group (**A**), the prediction with a set of normal-flesh juice (**B**) and the prediction with a set of translucent-flesh juice (**C**).

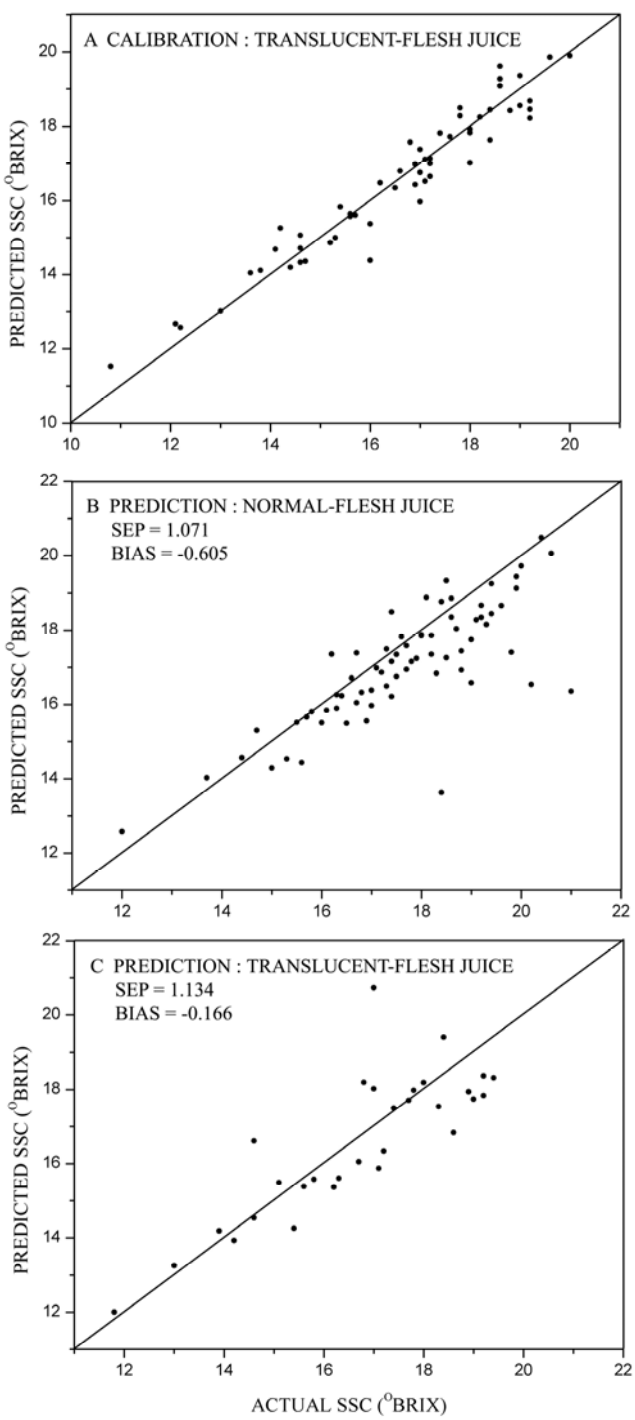

Fig. 5 Scatter plots of actual SSC and predicted SSC for the calibration set of translucent-flesh juice group (**A**), the prediction with a set of normal-flesh juice (**B**) and the prediction with a set of translucent-flesh juice (**C**).

the group of normal-flesh juice and the group of translucent-flesh juice are shown in **Fig. 3**. The second-derivative technique was used to process NIR absorbance data for analysis.

PLS calibration models were established for mangosteen juice using the second-derivative preprocessing data. **Table 2** shows the results of calibration and prediction for PLS models of normal-flesh juice, translucent-flesh juice and combined juice. The calibration model of normal-flesh juice was suitable for prediction of its own sample set (SEP = 0.655 and bias = 0.047) but the lowest performance was obtained for prediction with translucent-flesh juice set (SEP = 1.245 and bias = 0.224). The calibration model of translucent-flesh juice was unsuitable for prediction of both normal-flesh juice set (SEP = 1.071 and bias = -0.605) and its own sample set (SEP = 1.134 and bias = -0.166). The calibration model of combined juice showed the best performance for prediction of normal-flesh juice set (SEP = 0.553 and bias = 0.052) but gave poorer performance for prediction of translucent-flesh juice set (SEP = 1.027 and bias = 0.122).

Therefore, all of the prediction sets of translucent-flesh juice set obtained poor accuracy when using all calibration models for prediction. **Fig. 4** shows the performance of the normal-flesh juice calibration model for SSC prediction. The prediction accuracy was satisfied when normal-flesh juice set was used for the prediction. On the other hand, the prediction accuracy was unsatisfied when translucent-flesh juice set was used for the prediction. **Fig. 5** presents the performance of the translucent-flesh juice calibration model for SSC prediction. The prediction accuracy was unsatisfied when both normal-flesh juice set and translucent-flesh juice

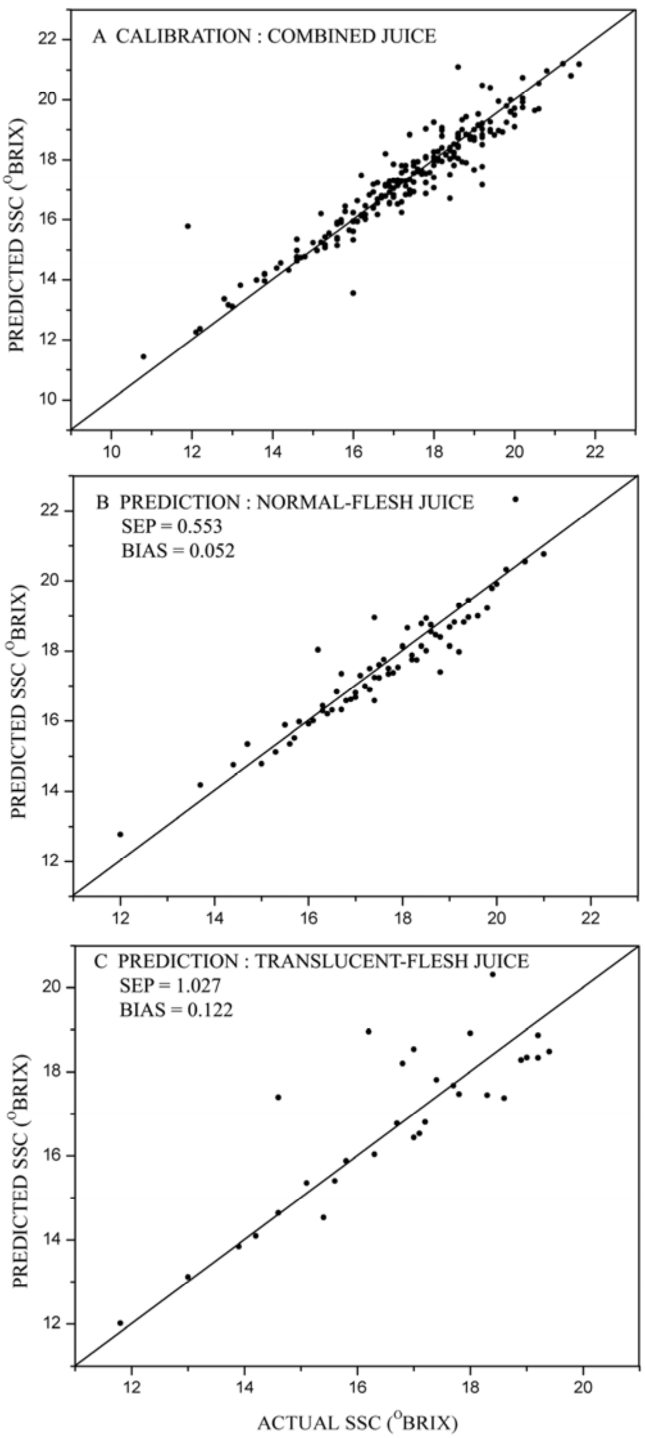

Fig. 6 Scatter plots of actual SSC and predicted SSC for the calibration set of combined juice group (**A**), the prediction with a set of normal-flesh juice (**B**) and the prediction with a set of translucent-flesh juice (**C**).

set were used for the prediction. **Fig. 6** also shows the performance of the combined juice calibration model for SSC prediction. The prediction accuracy was satisfied when normal-flesh juice set was used for the prediction but the prediction accuracy was unsatisfied when translucent-flesh juice set was used for the prediction. Therefore, a high accuracy of prediction could be obtained when calibration model of normal-flesh juice was used for prediction of normal-flesh juice set. On the other hand, translucent-flesh juice set obtained poor accuracy when tested with all calibration models.

CONCLUSION

The calibration model of mangosteen juice can be used to accurately predict SSC of mangosteen juice. A calibration model of combined juice or the normal-flesh juice could be developed by the second-derivative preprocessing data and used for the prediction. The accuracy of the prediction was high when the prediction set was the normal-flesh juice. The accuracy of the prediction obtained was poor when the prediction set was the translucent-flesh juice. All of calibration models were unsatisfied to use for prediction of the translucent-flesh juice set. It is interesting that this result is a possible way to obtain an improved technique for practical application of on-line sorting systems. Thereby, this method could be applied to discriminate between normal mangosteens and translucent mangosteens in the future.

ACKNOWLEDGEMENTS

The authors acknowledge the support of the Faculty of Agro-Industry, King Mongkut's Institute of Technology Ladkrabang and would also like to thank Kasetsart Agricultural and Agro-Industrial Product Improvement Institute for their kind technical help and use of their laboratory.

REFERENCES

Dull GG, Birth GS, Smittle DA, Leffler RG (1989) Near infrared analysis of soluble solids in intact cantaloupe. *Journal of Food Science* **54**, 393-395

Dull GG, Leffler RG, Birth GS, Smittle DA (1992) Instrument for non-destructive measurement of soluble solids in honeydew melons. *Transactions of the American Society of Agricultural Engineers* **35**, 735-737

Kawano S, Watanabe H, Iwamoto M (1992) Determination of sugar content in intact peaches by near infrared spectroscopy with fiber optics in interacttance mode. *Journal of the Japanese Society for Horticultural Science* **61**, 445-451

Kawano S, Fujiwara T, Iwamoto M (1993) Non-destructive determination of sugar content in satsuma mandarin using near infrared (NIR) transmittance. *Journal of the Japanese Society for Horticultural Science* **62**, 465-470

Martin FW (1980) Durian and mangosteen. In: Nagy S, Shaw PE (Eds) *Tropical and Subtropical Fruits: Composition, Properties and Uses*, The AVI Publishing, Westport, CT, pp 407-414

McGlone VA, Kawano S (1998) Firmness, dry-matter and soluble-solids assessment of postharvest kiwifruit by NIR spectroscopy. *Postharvest Biology and Technology* **13**, 131-141

Pankasemsuk T, Garner Jr. JO, Matta FB, Silver JL (1996) Translucent flesh disorder of mangosteen fruit (*Garcinia mangostana* L.). *The American Society for Horticultural Science* **31**, 112-113

Peirs A, Tirry J, Verlinden B, Darius P, Nicolai BM (2003) Effect of biological variability on the robustness of NIR models for soluble solids content of apples. *Postharvest Biology and Technology* **28**, 269-280

Saranwong S, Sornsrivichai J, Kawano S (2003) Performance of a portable NIR instrument for brix value determination of intact mango fruit. *Journal of Near Infrared Spectrosc*opy **11**, 175-181

Slaughter DC, Thompson JF, Tan ES (2003) Nondestructive determination of total and soluble solids in fresh prune using near infrared spectroscopy. *Postharvest Biology and Technology* **28**, 437-444

Sohn MR, Kwon YK, Cho RK (2001) Development of robust calibration for determination sweetness of Fuji apple fruit using near infrared reflectance spectroscopy. *Near Infrared Analysis* **2 (1)**, 55-58

Teerachaichayut S, Kil KY, Terdwongworakul A, Thanapase W, Nakanishi Y (2007) Non-destructive prediction of translucent flesh disorder in intact mangosteen by short wavelength near infrared spectroscopy. *Postharvest Biology and Technology* **43**, 202-206

Ventura M, de Jager A, de Putter H, Roelofs FPMM (1998) Non-destructive determination of soluble solids in apple fruit by near infrared spectroscopy (NIRS). *Postharvest Biology and Technology* **14**, 21-27